

PRELIMINARY PETROLOGICAL STUDIES OF THE METAMORPHIC ROCKS OF THE EASTERN SØR RONDANE MOUNTAINS

Edward S. GREW¹, Masao ASAMI² and Hiroshi MAKIMOTO³

¹*Department of Geological Sciences, University of Maine,
Orono, Maine 04469, U.S.A.*

²*Department of Geological Sciences, College of Liberal Arts, Okayama
University, 1-1, Tsushima-naka 2-chome, Okayama 700*

³*Geological Survey of Japan, 1-3, Higashi 1-chome, Tsukuba 305*

Abstract: The eastern Sør Rondane Mountains is largely underlain by biotite and biotite-hornblende quartzo-feldspathic gneisses, in which six rock types occur as lenses ranging from <1 m to >1 km in extent: (1) manganese quartzite and iron-rich mafic granulite (2) mafic granulites and amphibolites, (3) ultramafics, (4) garnet-biotite and biotite gneisses, (5) marble and calc-silicate rocks, and (6) cummingtonite ± orthopyroxene orthogneiss. Distinctive mineral assemblages include plagioclase — K-feldspar — fayalite — hedenbergite/augite — ferrosilite — ferro-pargasitic hornblende—almandine—ilmenite—magnetite—graphite—allanite—pyrrhotite in iron-rich mafic granulite, quartz—spessartine—pyroxmangite—manganoan pigeonite—manganoan augite—manganoan ilmenite (+ pyrophanite)—tirodite (secondary) in a manganese quartzite, pyropic garnet—biotite—clinopyroxene—hornblende—anorthite in mafic granulite, sillimanite—garnet—spinel ± corundum (no cordierite) in garnet-biotite gneiss, and forsterite—spinel—calcite and forsterite—diopside—calcite—dolomite in marbles. Secondary minerals include clinohumite, geikielite and Mg-allanite in marble and margarite and högbomite in amphibolite. Kyanite relics are found in plagioclase in metapelite and with gedrite in garnet in a biotite ± spinel ± corundum schist; these imply pressures above 4 kbar on the prograde path. Pressures and temperatures calculated from mineral compositions are ≥7 kbar and 700–750°C for an early granulite facies event and 500–600°C for a later, discrete amphibolite facies event. Introduction of rare elements during the latter event and subsequent retrogression in the greenschist facies resulted in the local development of tourmaline, fluorite, allanite (in part) and a mineral of the zirconolite group.

1. Introduction

The eastern Sør Rondane Mountains (Fig. 1) is underlain largely by high grade metamorphic rocks belonging to the Precambrian shield of East Antarctica. The present paper summarizes petrological studies of samples collected in the eastern Sør Rondane Mountains during the 29th JARE. These studies focussed on ten samples of special mineralogical and petrologic interest. For a more general account of the geology, the reader is referred to ASAMI *et al.* (1989).

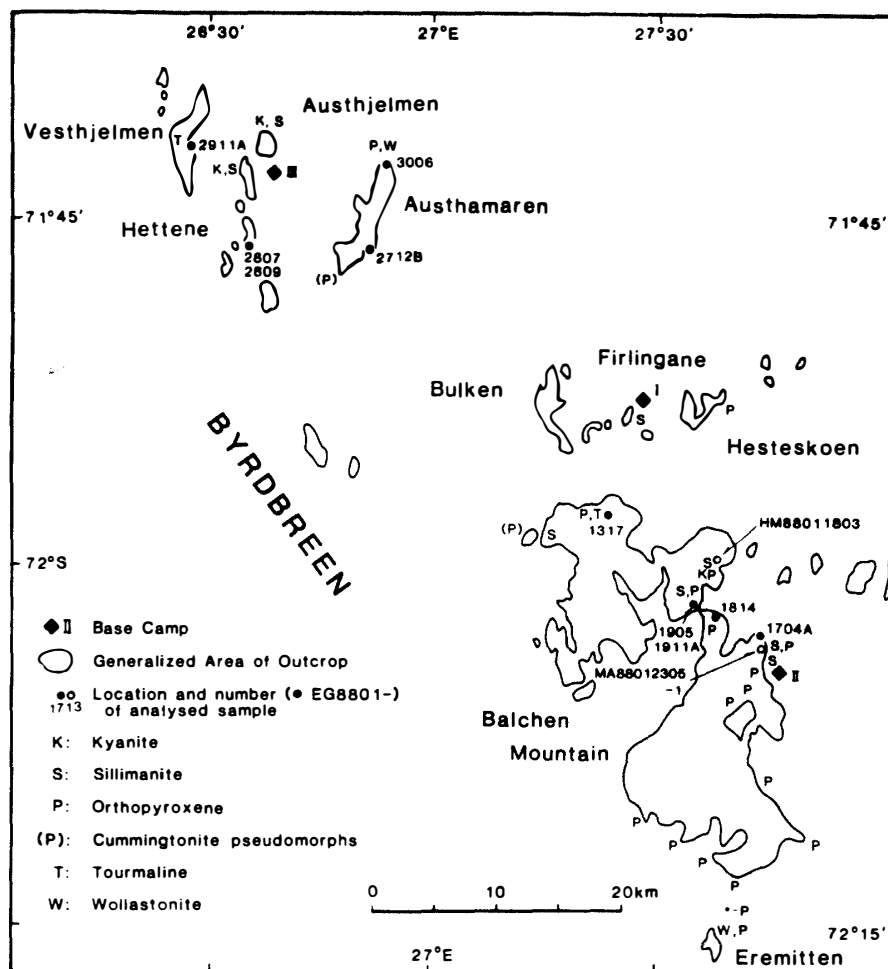


Fig. 1. Map of mineral and sample localities in the eastern Sør Rondane Mountains. The cummingtonite pseudomorphs are presumed to have formed from orthopyroxene.

2. Description of the Distinctive Rock Types

The dominant metamorphic rocks are biotite and biotite-hornblende quartzo-feldspathic gneisses, commonly well-layered. Leucocratic varieties appear migmatitic in the field. Quartz, plagioclase, microcline, biotite, and hornblende are present in most sections, typical accessories are opaques, zircon, apatite, and allanite. Less common are garnet, clinopyroxene, and sphene. Among secondary minerals, chlorite, muscovite, and calcite are ubiquitous, epidote is less common. In the southern part of Balchen Mountain (=Balchenfjella) and Eremitten, the quartzo-feldspathic gneisses are commonly weathered yellow instead of gray or pink, as are the gneisses further north. These charnockitic rocks contain orthopyroxene or cummingtonite derived from retrogression of orthopyroxene.

A wide variety of distinctive rock types form concordant to subconcordant lenses in the quartzo-feldspathic gneisses. These lenses range from less than a meter to several tens of meters thick and up to a kilometer or more in length. Rock types include (1) manganese quartzite and iron-rich mafic granulite, (2) mafic granulites and amphibolites, (3) ultramafic rocks, (4) garnet-biotite and biotite gneisses, (5)

marble and calc-silicate rocks, (6) cummingtonite±orthopyroxene orthogneiss.

2.1. *Manganese quartzite and iron-rich mafic granulite*

At Hettene, a rusty-weathering quartzitic unit includes a layer 0.5 m thick unusually enriched in manganese, as well as graphitic biotite-garnet gneiss and hornblende-biotite gneiss. Typically the quartzite contains spessartine, manganoan actinolite, biotite, and manganoan ferroan dolomite (EG88012809, Tables 1 and 2). Pentlandite has exsolved from pyrrhotite in sample EG88012809. In this layer are pods a few cm thick of black-weathering, green cherty quartzite containing spessartine, pyroxmangite, Mn-rich pyroxenes (pigeonite, augite), ilmenite, rare pyrophanite, tirodite (forming from pyroxenes), pyrrhotite, and chalcopyrite; rhodochrosite forms

Table 1. *List of minerals from the eastern Sør Rondane Mountains and their abbreviations (adopted from KRETZ, 1983).*

Act	actinolite	Ilm	ilmenite
Aln	allanite	(Jo)	johannsenite) ¹
Alm	almandine	(Ka)	kanoite) ¹
Ann	annite	Kfs	K feldspar
Ap	apatite	Ky	kyanite
Bt	biotite	Mag	magnetite
Cam	Ca clinoamphibole	Mrg	margarite
Cpx	Ca clinopyroxene	Mnz	monazite
Cal	calcite	Ms	muscovite
Ccp	chalcopyrite	Ol	olivine
Chl	chlorite	Opx	orthopyroxene
Chu	clinohumite	Prg	pargasite
Czo	clinozoisite	Phl	phlogopite
Crn	corundum	Pgt	pigeonite
Cum	cummingtonite	Pl	plagioclase
Di	diopside	Prh	prehnite
Dol	dolomite	Prn	pyrophanite
En	enstatite	Py	pyrite
Ep	epidote	Prp	pyrope
Fst	fassaite	Pxm	pyroxmangite
Fa	fayalite	Po	pyrrhotite
Fs	ferrosilite	Rds	rhodochrosite
Fl	fluorite	Rdn	rhodonite
Fo	forsterite	Rt	rutile
Ghn	gahnite	Scp	scapolite
Grt	garnet	Sil	sillimanite
Ged	gedrite	Sps	spessartine
Gkl	geikielite	Sp	sphalerite
Gr	graphite	Spn	sphene
Grs	grossular	Spl	spinel
Hd	hedenbergite	Tir	tirodite
Hc	hercynite	Tur	tourmaline
Hög	högbomite	Tr	tremolite
Hbl	hornblende	Wo	wollastonite
		Zrn	zircon

¹ Minerals in parentheses were not found.

Table 2. Mineralogy of the analyzed samples.

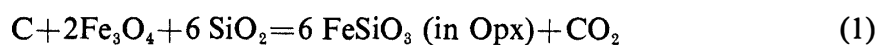
Type	Manganese quartzite		Mafic rocks; Amphibolites			Meta-pelite	Marble		Calc-silicate	
	2807	2809	3006	2911A	1317	1704A	1814	1911A	1905	2712B
EG8801-Qtz	X	X			x	X				
Kfs			X			x				x
Pl			X	X	X	X			X	
Scp									X	X
Ol			X				X	X		
Chu							x	x		
Cpx	X		X	x	x				X	X
Pyroxene	PGT		opx							
Hbl			X	X	X					X
Act		X			x			x	X	
Cum	TIR				CUM					
Bt		X	x	x	X	X	X	X		x
Mica				mrg					ms	ms
Chl		x		x			x	x		x
Grt	X	X	X		X	X				
Czo				x					X	x
Aln	x		x	x			x			x
Spn	x			x						x
Zrn			x	x		x	x		x	x
Ap	X	x	x	x	x		x	x		
Cal				x			X	X	X	X
Dol		x					x	x		
Mag			x	X		X		x		
Ilm	x		x	X		X	x	x		
Rt				x		x		x		
Spl				x	x	X	X	X		
Hög				x		x				
Sulfide	x	x	x	x			x	x		
Other	rds prn PXM		gr			SIL		zirono- lite (?)	fl prh	fl

X, PGT: major constituent; x, mrg: minor constituent. In mineral list, only one member of Fe-Mg isomorphous series is given.

isolated grains and microveinlets (EG88012807, Figs. 2 and 3).

At the north end of Austhamaren, an iron-rich mafic granulite (EG88013006) together with garnetiferous granulites and a marble underlies cummingtonite ± orthopyroxene orthogneiss (see below). The equilibrium mineral assemblage in EG88013006 is inferred to be Pl-Kfs-Fa-Cpx-Fs-Hbl-Alm-Ilm-Mag-Gr-Aln-Po (Fig. 4, mineral abbreviations listed in Table 1, compare with KATSUSHIMA, 1985).

The Gr-Mag association may have been stabilized by the absence of quartz:



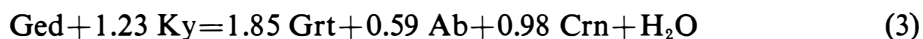
We infer a metasedimentary origin for not only the Mn-rich quartzite, but also the iron-rich mafic granulite, despite the latter's similarity to other Hbl-rich mafic granulites.

2.2. *Mafic granulites and amphibolites*

Mafic granulites and amphibolites which are the most widespread of the subordinate rock types, differ from the host quartzo-feldspathic gneiss in the greater proportion of mafics and in the absence or scarcity of quartz and K-feldspar. The mafic granulites and amphibolites are compositionally and mineralogically a heterogeneous group, but all appear to have a magmatic parentage. Garnetiferous varieties are common, while ortho- and clinopyroxenes are important constituents as far north as 72°S, for example, the prominent "Kuroiwa" Pl-Hbl-Cpx-Opx±Grt metagabbro in a body nearly 1 kilometer long located 6 km northwest of Camp II. A mafic lens from northwest Balchen contains abundant spinel (assemblage Pl-Hbl-Spl-Cpx±Bt). The two samples selected for analyses, EG88011317 and -2911A, are texturally complex. In EG88012911A, "fassaite" and hornblende form vermicules in coarse anorthite laths (Fig. 5), suggesting a symplectitic intergrowth. Sample EG88011317 is layered. One part of the analyzed thin section contains cumingtonite, intermediate plagioclase, and minor quartz, while another layer contains biotite, garnet, plagioclase, and minor hornblende. Most of the section is garnet amphibolite with embayed clinopyroxene relics, plagioclase, minor biotite and anorthite-pargasite±hercynite symplectites around garnet (Fig. 6).

2.3. *Ultramafic Rocks*

Ultramafic rocks are similar in mineralogy to the mafic rocks, but lack feldspar. At three localities in Balchen Mountain, one near Base Camp II and the others 8 km (sample locality as EG88011905, -1911A) and 10 km (S, P, K) northwest of it (Fig. 1), are olivine-rich lenses containing minor orthopyroxene, chrome spinel, and secondary talc. Reaction zones of biotite and amphiboles have developed between these lenses and the host quartzo-feldspathic gneisses. At the northernmost locality, the reaction zone includes a biotite-plagioclase-garnet schist containing spinel, corundum and rare sillimanite. This schist is probably a pelitic rock modified by interaction with the ultramafic. Rutile, biotite and rare kyanite, gedrite, and quartz occur as microscopic inclusions in the garnet porphyroblasts (sample HM88011803D). Simplified equations for Mg-enrichment in garnet by reactions of the included phases (Ged composition given in Section 3. Mineralogy) are:



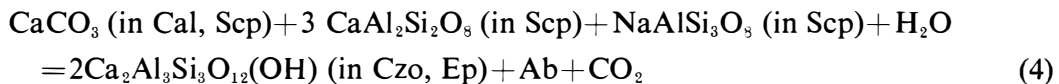
2.4. *Garnet-biotite and biotite gneisses*

Rocks of pelitic composition are typically quartzo-feldspathic gneisses containing garnet, biotite, sillimanite, and monazite; locally also graphite. These rocks are rare except at the sillimanite localities immediately north of Camp II, where layers of migmatitic pelitic gneiss are up to 3 m thick. In these migmatites, sillimanite, garnet, biotite, hercynite, magnetite, and, locally, corundum are enriched in cm-thick layers in a quartzo-feldspathic matrix (e.g. EG88011704A). Zinc enrichment in a layer a few cm thick associated with garnet-biotite gneiss has stabilized the assemblage Ghn-Qtz-Bt-Grt-Pl-Sp-Mnz-Po-Py-Ccp (MA88012305-1, compare FROST, 1973). An

undersaturated feldspathic rock contains Kfs-Pl-Bt-Crn-Rt-Ilm-Po-Py-Ccp. Garnetiferous biotite gneisses from Hettene and Austhjelmene contain fibrolite and kyanite, the latter as rare, rounded relics enclosed in plagioclase (Fig. 7).

2.5. *Marble and calc-silicate rocks*

Marble and calc-silicate rocks form lenses up to 10 m thick and are most abundant in a band extending northwest across the northern part of Balchen Mountain (GREW *et al.*, 1988). One type of marble (in part dolomitic) contains primary forsterite, diopside, spinel, and/or graphite, *e.g.* Fo-Spl-Cal-Phl (EG88011814, -1911A, Table 2) and Di-Fo-Cal-Dol-Gr. Another type of marble contains quartz, K-feldspar, scapolite, sphene, clinopyroxene and/or grossular. During a later metamorphic event, when aqueous fluids, locally carrying rare metals, were introduced, tremolite, chlorite, clinohumite, Mg-rich allanite, a zirconolite-group mineral, magnetite, ilmenite-geikielite formed by reactions among forsterite, spinel, and phlogopite (compare HIROI and KOJIMA, 1988), while plagioclase, epidote and grossular formed by reaction of scapolite and calcite (Fig. 8), for example:



Metasomatism of the marble accompanied pegmatites or developed along fractures, resulting in veins of calc-silicate minerals, of which EG88011905 is an example. In this sample, the core of the vein is largely scapolite with minor clinzoisite (Fig. 9), muscovite, calcite, and prehnite; the margin, diopside with minor actinolite. Anorthite relics are enclosed in scapolite near the diopside zone. Sample EG88012712B, which was collected from an isolated lens 1 × 2 m across in biotite-hornblende gneiss, appears also to be metasomatic in origin. Rare earth mineralization in this sample resulted in allanite selvages between scapolite and calcite (Fig. 10); these probably formed by a reaction analogous to (4) involving introduced rare earth elements.

Well-layered calc-silicate rocks are presumed to be isochemically recrystallized calcareous sediments. Examples include two wollastonite rocks (Fig. 1): Wo-Cpx-Scp-Grs-Spn-Qtz from Eremitten (Fig. 11, MA88012206-1) and a similar assemblage lacking Scp from Austhamaren. Minor calcic plagioclase is also present in the Eremitten calc-silicate, suggesting that the rock may have been subjected to conditions approaching those for the reaction $\text{Wo} + \text{An} = \text{Grs} + \text{Qtz}$ during its metamorphic evolution.

2.6. *Cummingtonite ± orthopyroxene orthogneiss*

Cummingtonite ± orthopyroxene orthogneiss crops out at the north end of Austhamaren, where relics of orthopyroxene are preserved in cummingtonite-calcic clin amphibole pseudomorphs with hornblende margins in a dominantly plagioclase matrix (Fig. 12). A particularly coarse-grained variety contains masses of fresh orthopyroxene with stout lamellae of clinopyroxene in a texture similar to that resulting from inversion of pigeonite (Fig. 13, compare BONNICHSEN, 1969). The orthogneiss is cut by several metamorphosed dikes enriched in garnet. This pyroxene texture

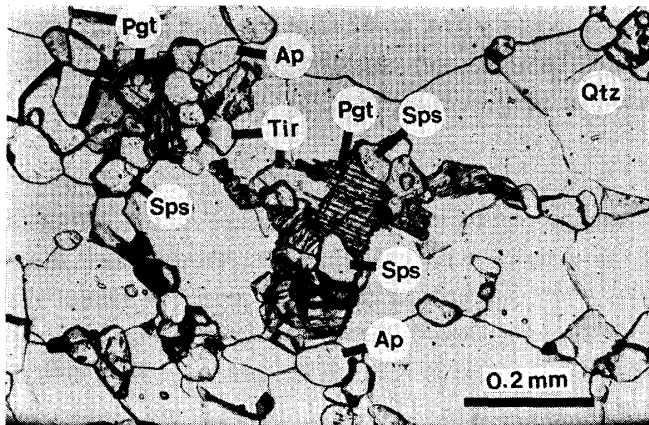


Fig. 2. Photomicrograph of cherty manganese quartzite EG88012807. Plane light. Tirodite (Tir) is replacing pigeonite (Pgt).

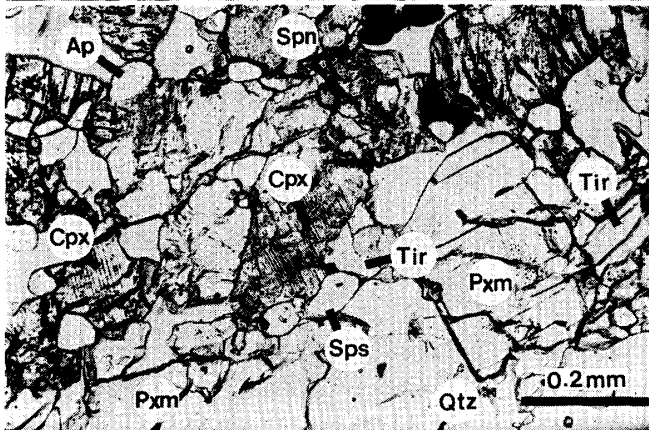


Fig. 3. Photomicrograph of cherty manganese quartzite EG88012807. Plane light. Pyroxmangite grains (Pxm) are clean, while the striated clinopyroxene grains (Cpx) are turbid.

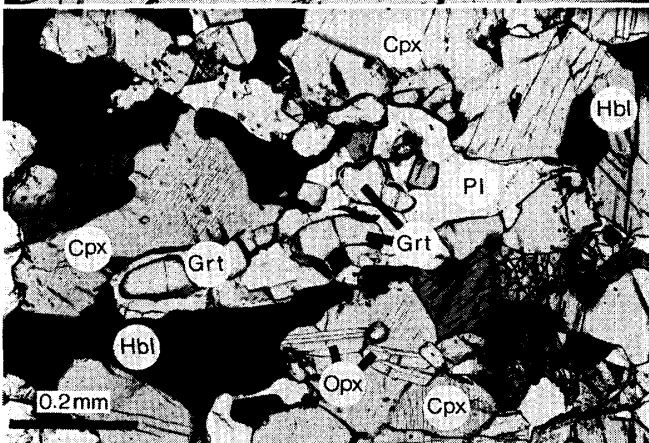


Fig. 4. Photomicrograph of iron-rich mafic granulite, EG88013006. Plane light. Ferrosilite (Opx) lamellae are intergrown with hedenbergite-augite (Cpx) showing exsolution lamellae.

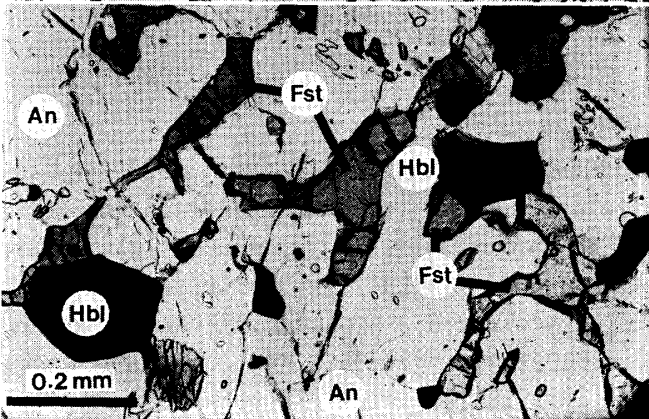


Fig. 5. Photomicrograph of amphibolite, EG88012911A. Plane light. Fassaite grains (Fst) have curved outlines suggestive of a symplectitic intergrowth with anorthite (An).

Fig. 6. Photomicrograph of garnet amphibolite, EG88011317. Plane light. Clinopyroxenes (Cpx) are finely striated and embayed. Garnet (Grt) is embayed by hornblende-plagioclase symplectite. A few hornblende grains are zoned (indicated by Z).

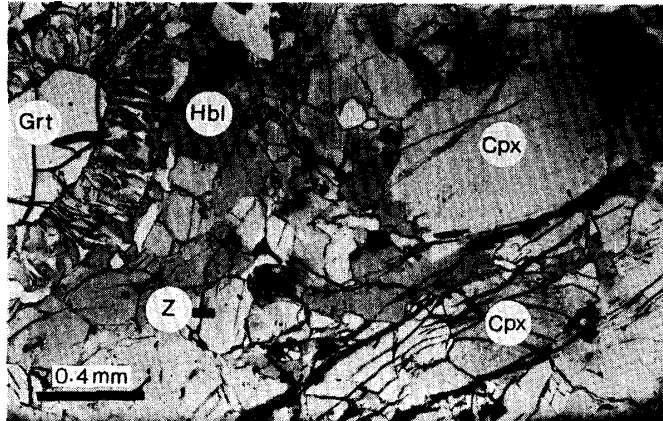


Fig. 7. Photomicrograph of biotite gneiss from nunatak between Hettene and Austhjelmen, HM-88012803D. Plane light. Kyanite (Ky) relics in plagioclase (Pl).

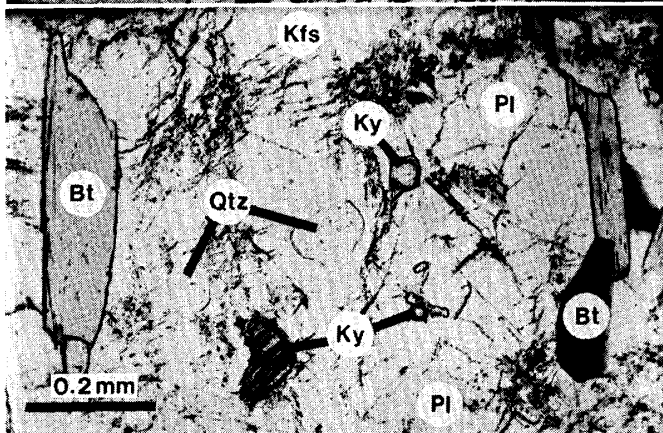


Fig. 8. Photomicrograph of marble from Balchen Mountain EG-88011920A (near locality for EG-88011905, -1911A). Plane light. Some scapolite (Scp) in direct contact with calcite (Cal), other separated by selvage of epidote (Ep), locally with plagioclase (Pl).

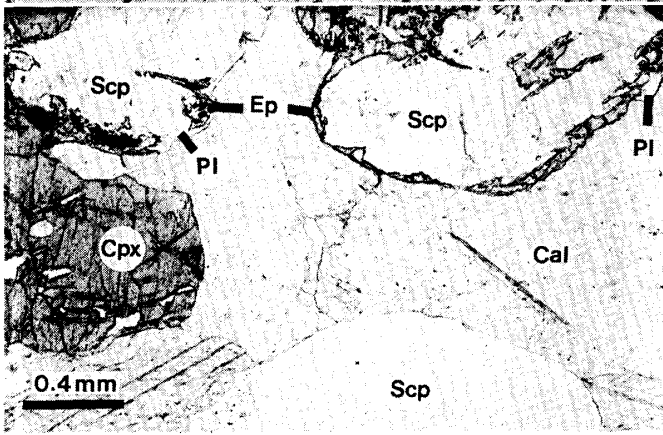
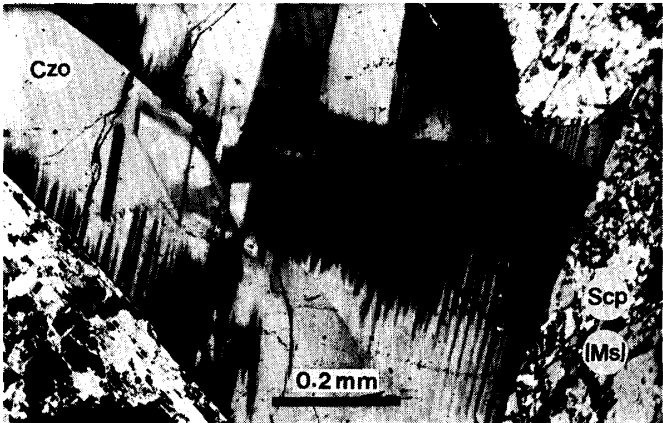


Fig. 9. Photomicrograph of calc-silicate rock from Balchen Mountain, EG88011905. Crossed nicols. Polysynthetically twinned clinzoisite (Czo) in matrix of scapolite (Scp) partly altered to muscovite (Ms).



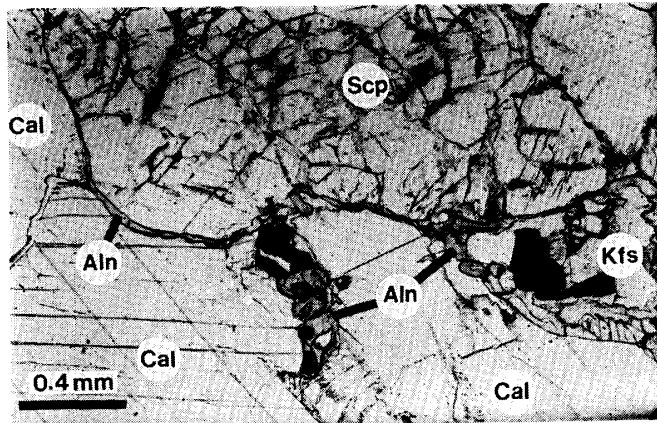


Fig. 10. Photomicrograph of calc-silicate rock, EG88012712B. Plane light. Selvage of allanite (Aln) between calcite (Cal) and scapolite.

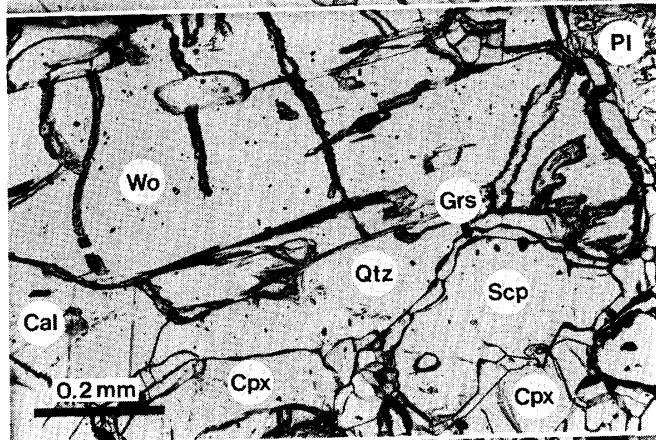


Fig. 11. Photomicrograph of calc-silicate granulite from Eremitten, MA88012206-1. Plane light. Wollastonite (Wo), calcite (Cal), and quartz (Qtz) are in mutual contact (3-way junction partially obscured by hole left-center of photograph). Scapolite (Scp) surrounded by selvage of grossular (Grs). Area marked Pl is symplectite of calcic plagioclase and scapolite.

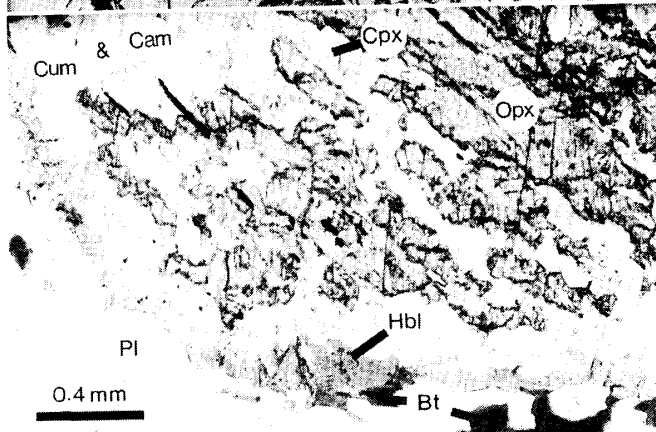


Fig. 12. Photomicrograph of cummingtonite-orthopyroxene orthogneiss, EG88013013B (same locality as EG88013006). Plane light. Relict orthopyroxene (Opx) and subordinate clinopyroxene (Cpx) in pseudomorph consisting largely of a pale cummingtonite — Ca clinoamphibole aggregate (Cam + Cum), with patches of green hornblende (Hbl), generally at margin of the aggregate.

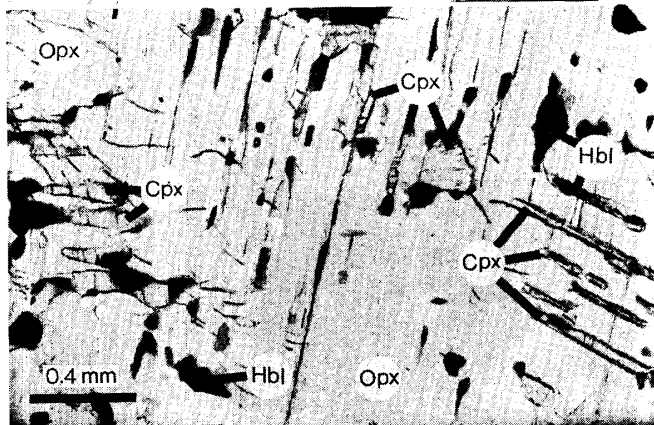


Fig. 13. Photomicrograph of a single orthopyroxene grain (Opx) with lamellae of clinopyroxene (Cpx) and hornblende (Hbl) from Austhamaren, EG88013011 (same locality as EG88013006). The differing orientation of the clinopyroxene lamellae suggests that these are derived from exsolution of pigeonite grains that subsequently inverted to orthopyroxene (compare with BONNICHSEN, 1969, Fig. 11 and 14).

and abundance of dikes suggest that the orthogneiss and associated dikes could be part of a premetamorphic plutonic complex intrusive into calcareous and iron-rich sediments. Quartz-plagioclase-biotite±garnet rocks with cummingtonite knots or orthopyroxene are found at the northwest corner of Balchen Mountain, southern Austhamaren and southern Balchen Mountain (Fig. 1). These rocks are similar to the orthogneiss of northern Austhamaren and may represent a rock type distinct from other charnockitic rocks.

Deformed metadikes consisting of a fine-grained biotitic schist locally with abundant sphene, are found sparingly throughout the eastern Sør Rondane Mountains (GREW *et al.*, 1988; ASAMI *et al.*, 1989). Our observations suggest that the biotitic schist metadikes are younger than the granulite-facies metamorphism, while the Austhamaren orthogneiss and associated garnet-rich metadikes appear to be older.

3. Mineralogy

The minerals described below have been analyzed with the JEOL JXA 733 elec-

Table 3. Compositions of plagioclases and scapolite.

Sample	3006	2911A	1317		1905		2712B
Mineral	Pl	Pl	Pl ¹	Pl ²	Pl	Scp	Scp
SiO ₂	65.20	42.57	43.21	54.44	44.29	45.04	48.05
TiO ₂	0	0	0	0	0	0	0
Al ₂ O ₃	21.02	36.74	36.08	28.36	35.56	27.97	25.96
Cr ₂ O ₃	<0.01	0.02	0	0	0.01	0	0
FeO	0.16	0.09	0.09	0.13	0.07	0.07	0.10
MnO	0.01	0	0.04	<0.01	0	0	0
MgO	0	0	0	0.06	0	0.02	0
CaO	2.17	19.70	19.81	10.64	18.67	18.02	16.16
Na ₂ O	10.67	0.07	0.64	5.86	0.75	3.39	4.78
K ₂ O	0.22	0.01	0	0.02	0	0.27	0.53
ZnO	—	0.16	—	—	0.10	0.19	0.11
Total	99.46	99.37	99.87	99.51	99.46	94.97	95.96
Cations per 8 oxygens				Al+Si=12			
Si	2.889	1.986	2.008	2.470	2.056	6.929	7.332
Ti	0	0	0	0	0	0	0
Al	1.098	2.020	1.976	1.516	1.946	5.071	4.668
Cr	0	0.001	0	0	0	0	0
Fe	0.006	0.003	0.004	0.005	0.003	0.009	0.013
Mn	0	0	0.001	0	0	0	0
Mg	0	0	0	0.004	0	0.005	0
Ca	0.103	0.985	0.986	0.517	0.928	2.971	2.642
Na	0.917	0.007	0.057	0.515	0.068	1.012	1.415
K	0.012	0.001	0	0.001	0	0.052	0.102
Zn	—	0.006	—	—	0.003	0.022	0.013
Total	5.026	5.008	5.033	5.030	5.005	16.070	16.185
X _{Ca}	0.101	0.993	0.945	0.501	0.932	0.746	0.651

¹ With Hc. ² With Cum.

Table 4. Compositions of olivines and clinohumite.

Sample	3006	1814	1911A	1814	1911A
Mineral	Fa	Fo	Fo	Chu	Chu
SiO ₂	29.44	41.09	41.21	36.32	37.78
TiO ₂	0	0.02	0	2.65	2.69
Al ₂ O ₃	0.01	0	0	0.04	0.03
Cr ₂ O ₃	0	0	0.02	<0.01	0
FeO	67.75	3.38	3.98	2.78	3.84
MnO	0.87	0.10	0.21	0.08	0.17
MgO	1.04	55.96	55.27	54.52	54.15
CaO	0.01	0	0.01	0	0.01
Na ₂ O	0	0.02	0.02	0.02	0
K ₂ O	0.01	0.01	0.02	0.02	0
Total	99.12	100.58	100.74	96.43	98.67
	Cations per 4 oxygens			17.2 oxygens ¹	
Si	0.999	0.975	0.979	3.895	3.968
Ti	0	0	0	0.214	0.212
Al	0	0	0	0.004	0.004
Cr	0	0	0	<0.001	0
Fe	1.923	0.067	0.079	0.249	0.338
Mn	0.025	0.002	0.004	0.007	0.015
Mg	0.052	1.980	1.957	8.716	8.479
Ca	0	0	0	0	0.001
Na	0	0.001	0.001	0.004	0
K	0	0	0.001	0.003	0
Total	3.001	3.025	3.021	13.092	13.018
X _{Mg}	0.027	0.967	0.961	0.972	0.962

¹ Estimated from the ideal formula $4[(\text{Mg}, \text{Fe})_2\text{SiO}_4] [(\text{Mg}, \text{Fe})_{1-x}\text{Ti}_x(\text{OH}, \text{F})_{2-2x}\text{O}_{2x}]$ (DEER *et al.*, 1982).

tron microprobe at the National Institute of Polar Research using the standard method of the institute and the BENCE-ALBEE correction procedure. Selected individual analyses are listed in Tables 3–13 and suitable individual analyses for some minerals plotted in Figs. 14–19. A few microprobe analyses were done by M. YATES at the University of Maine (method in YATES and HOWD, 1988).

Plagioclases are commonly zoned and variable in composition (Table 3). For example, in EG88012911A patches as sodic as An 28 are present in anorthite, An 96–99.7 (Table 3). In EG88011317 plagioclase in the amphibolite and biotite-rich layers is An 83–94, somewhat more sodic than that in symplectites (mostly An 91–98, rarely to An 60); plagioclase with cummingtonite is considerably more sodic (An 48–73).

Analyzed olivines are near end-member fayalite and forsterite (Table 4). Analyses of the pleochroic and twinned secondary mineral in the two marbles are closest to clinohumite in stoichiometry (Table 4).

Orthopyroxenes include magnesian enstatite in ultramafic rocks, intermediate (“hypersthene”) in mafic and charnockitic rocks, and iron-rich ferrosilite in

Table 5. Compositions of pyroxenes.

Sample	3006	3006	2807	2807	2807	2911A	1317	1905	2712B
Pyroxene	Opx	Cpx	Pxm	Cpx	Pgt	Fst ¹	Cpx ¹	Cpx	Cpx ¹
SiO ₂	45.93	47.34	46.92	50.30	48.79	42.04	48.80	55.11	53.88
TiO ₂	0.06	0.13	0	0.02	0.07	1.87	0.12	0.04	0
Al ₂ O ₃	0.19	0.73	0	0.14	0.04	12.53	6.91	0.27	0.75
Cr ₂ O ₃	0	0	0	0.03	0	0	0.05	0	0
FeO	48.91	28.28	16.84	10.78	17.71	8.59	8.44	1.28	1.35
MnO	0.74	0.38	28.11	9.14	19.67	0.12	0.07	0.11	0.11
MgO	2.85	2.45	4.22	10.12	10.15	9.14	14.63	18.23	17.41
CaO	0.69	19.39	3.53	18.14	2.54	23.76	19.25	25.13	26.82
Na ₂ O	0.11	0.37	0	0.09	0.05	0.05	0.83	0.14	0.16
K ₂ O	0.01	<0.01	0	0.01	0	<0.01	0.12	0	0
ZnO	—	—	—	—	—	0.05	—	0.14	0
Total	99.50	99.07	99.63	98.77	99.01	98.13	99.22	100.45	100.48
Cations per 6 oxygens									
Si	1.984	1.960	1.985	1.982	1.990	1.622	1.825	1.989	1.958
Al	0.010	0.036	0	0.007	0.002	0.378	0.175	0.011	0.032
Sum	1.994	1.996	1.985	1.989	1.992	2.000	2.000	2.000	1.990
Ti	0.002	0.004	0	0.001	0.002	0.054	0.003	0.001	0.000
Al	0.000	0.000	0	0.000	0.000	0.192	0.129	0	0
Cr	0.000	0.000	0	0.001	0.000	0.000	0.002	0	0
Fe	1.767	0.979	0.596	0.355	0.604	0.277	0.264	0.039	0.041
Mn	0.027	0.013	1.007	0.305	0.680	0.004	0.002	0.003	0.003
Mg	0.183	0.151	0.266	0.594	0.617	0.526	0.815	0.981	0.943
Ca	0.032	0.860	0.160	0.766	0.111	0.982	0.771	0.972	1.044
Na	0.009	0.030	0	0.007	0.004	0.004	0.060	0.010	0.011
K	0.001	0.000	0	0.001	0	0	0.006	0	0
Zn	—	—	—	—	—	0.001	—	0.004	0
Total	4.015	4.033	4.015	4.017	4.009	4.041	4.052	4.009	4.032
X _{Mg}	0.094	0.134	0.309	0.626	0.505	0.655	0.755	0.962	0.958

¹ Core of zoned grain.

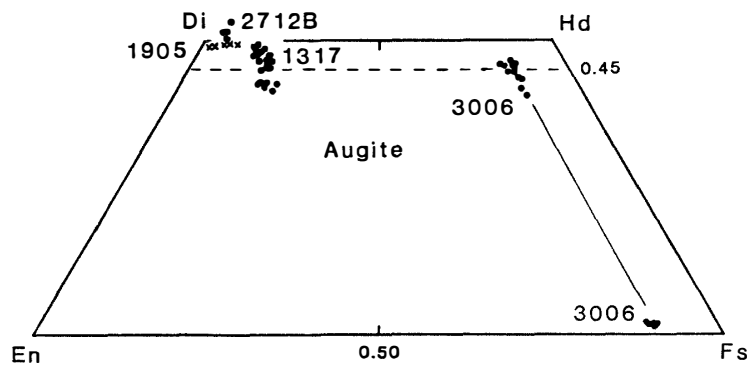


Fig. 14. Compositions of Mn-poor pyroxenes in terms of the pyroxene quadrilateral. × refers to sample (EG8801)1905. Pyroxenes containing less than 45% CaSiO₃ are augites (MORIMOTO et al., 1988).

EG88013006; only the last was analyzed (Table 5, Fig. 14). The ferrosilite in this sample forms small laths intergrown with hedenbergite (Fig. 4) and constitutes probably 1–2 modal % of the rock.

Calcic clinopyroxenes include nearly end-member diopside in calc-silicate rocks, hedenbergite-augite in the iron-rich rock, diopside-augite and “fassaite” (ferrian aluminous diopside in revised terminology, MORIMOTO *et al.*, 1988) in the mafic rocks (Table 5, Fig. 14). The hedenbergite-augite and diopside-augite contain abundant exsolution lamellae, which are probably the cause of variable Ca contents in the analyses. In addition, the diopside-augite and “fassaite” are compositionally heterogeneous in terms of Al_2O_3 (Tschermak substitution, Fig. 15).

Three pyroxene-like minerals occur in the Hettene cherty quartzite (EG88012807). On the basis of composition and relatively low optic axial angles, these have been provisionally identified as pyroxmangite, manganian pigeonite, and manganian calcic clinopyroxene (augite). Pyroxmangite forms relatively clear grains (Fig. 3) with rare twin lamellae and is compositionally relatively homogeneous (Figs. 16 and 17). Pigeonite is characterized by a prominent parting (Fig. 2) and local, fine ex-

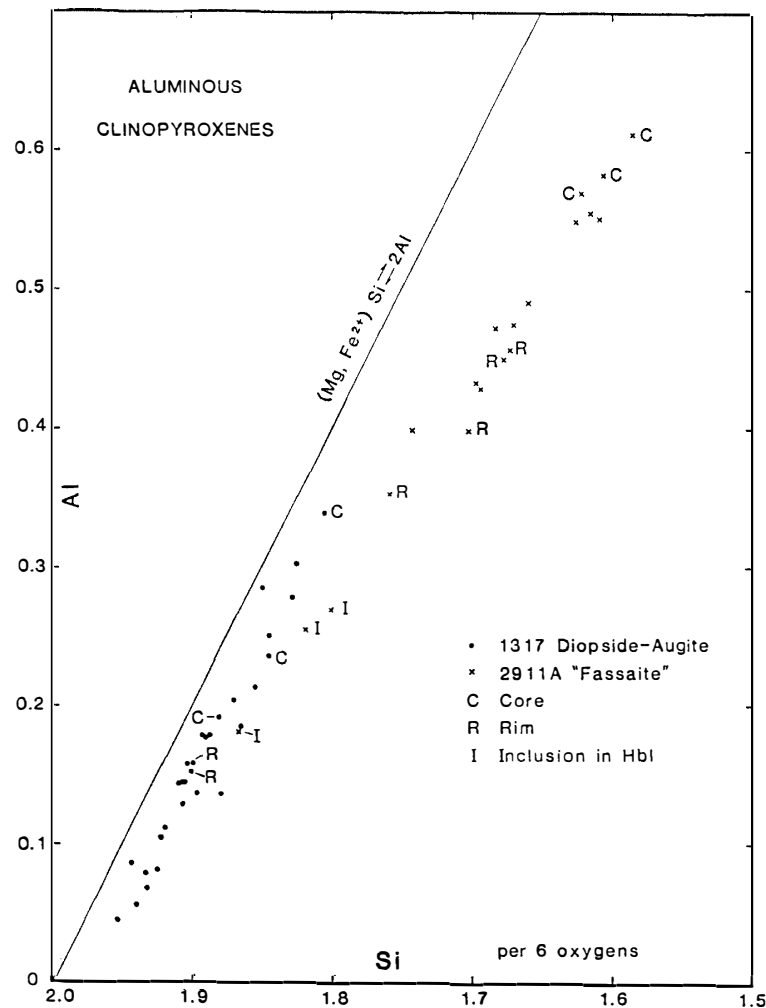


Fig. 15. Plot of compositions of aluminous clinopyroxenes for samples EG88011317 and EG88012911A. The line is for the ideal Tschermak substitution $(\text{Mg}, \text{Fe}^{2+})\text{Si} = 2\text{Al}$.

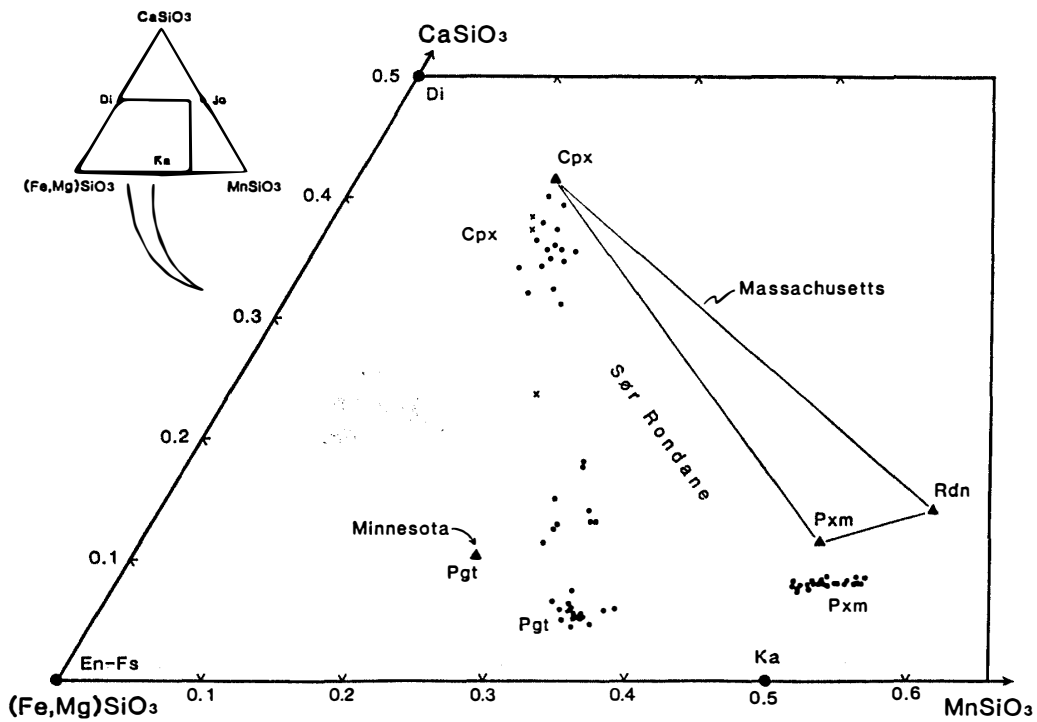


Fig. 16. Plot of pyroxene and pyroxenoid compositions in sample EG88012807, and comparison with compositions from Massachusetts (TRACY *et al.*, 1980) and Minnesota (BONNICHSEN, 1969). x-composition of presumed Cpx lamellae in pigeonite host.

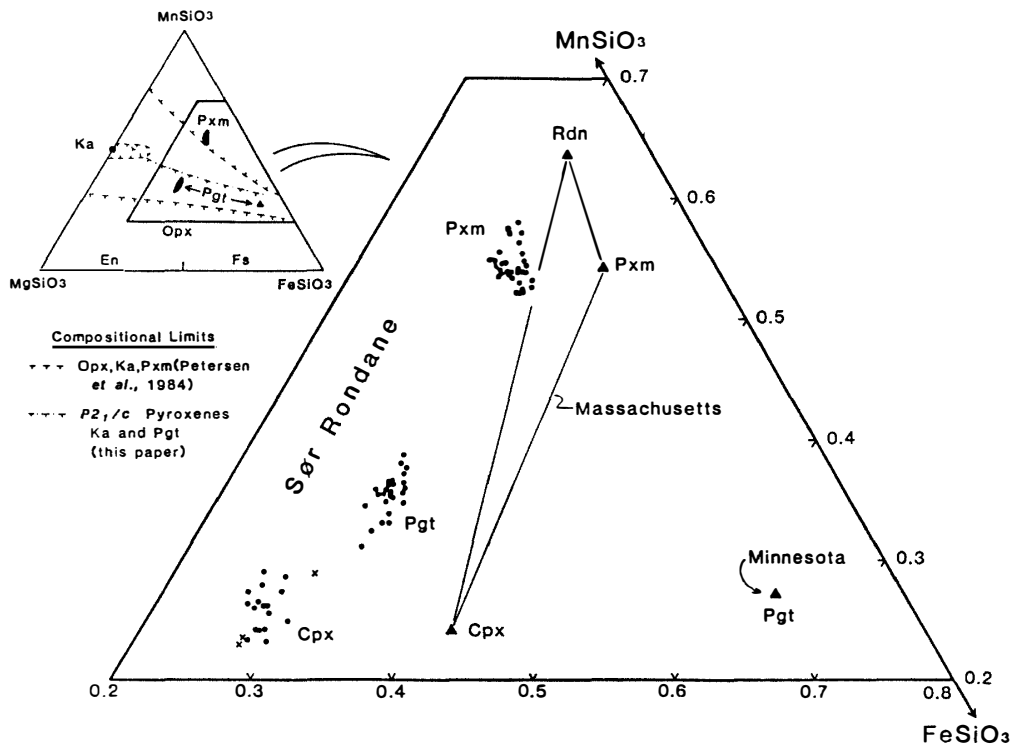


Fig. 17. Plot of pyroxene and pyroxenoid compositions in sample EG88012807 (neglecting CaSiO_3) x-composition of presumed Cpx lamella in pigeonite host. Compositional limits in index diagram are $X_{\text{Ca}} = \text{Ca}/(\text{Ca} + \text{Mg} + \text{Mn} + \text{Fe}) < 0.07$ (PETERSEN *et al.*, 1984), but $X_{\text{Ca}} \leq 0.10$ for the Minnesota Pgt, most Hettene Pgt and the Hettene Pxm.

solution lamellae. In one patch of the analyzed section, calcic clinopyroxene with abundant exsolution lamellae occurs with pyroxmangite and sphene (Fig. 3).

The Hettene pigeonite compositions plot between BONNICHSEN's (1969) manganian pigeonite from Minnesota and kanoite, ideally $\text{MgMnSi}_2\text{O}_6$ (KOBAYASHI, 1977, reported $\text{Mg}_{0.9}\text{Fe}_{0.1}\text{Mn}_{1.0}\text{Si}_2\text{O}_6$), thereby suggesting an extensive stability field for $P2_1/c$ pyroxenes in the CaSiO_3 -poor portion of the CaSiO_3 - MgSiO_3 - MnSiO_3 - FeSiO_3 system (Fig. 17). In contrast, PETERSEN *et al.* (1984) had predicted an extensive 2-phase field for Opx-Pxm, but only a restricted range of Fe/Mg ratios for kanoite. Prof. D. R. PEACOR of the University of Michigan, U.S.A., is currently studying the pyroxenes in the Hettene rock, and his results should lead to a better understanding of phase relations among Ca-Fe-Mg-Mn pyroxenes and pyroxmangite.

The compositions of coexisting augite and pyroxmangite are consistent (no crossing tie lines) with those reported by TRACY *et al.* (1980) from Massachusetts (Figs. 16 and 17). This implies similar conditions of formation, which are described as "near-granulite grade" by TRACY *et al.* (1980, p. 391).

Table 6. Compositions of miscellaneous amphiboles.

Sample	2807	2809	1317		1803D
	Tir	Act ¹	Mg-Hbl ²	Cum ²	Ged ³
SiO ₂	51.67	52.37	45.92	54.71	42.97
TiO ₂	0.09	0.08	0.48	0.02	0.49
Al ₂ O ₃	0.09	3.03	11.12	0.71	19.14
Cr ₂ O ₃	0	0.02	0.11	0	0.06
FeO	18.93	10.19	10.06	17.61	12.16
MnO	11.93	2.60	0.12	0.34	0.00
MgO	12.65	17.17	15.74	23.42	19.46
CaO	1.53	10.57	11.36	0.36	0.41
Na ₂ O	0	0.54	1.41	0.09	2.15
K ₂ O	0	0.15	0.16	0.02	0.02
Total	96.89	96.70	96.47	97.27	96.86
Cations per 23 oxygens					
Si	7.920	7.600	6.686	7.810	6.092
Al	0.016	0.400	1.314	0.120	1.908
Sum	7.936	8.000	8.000	7.930	8.000
Ti	0.010	0.009	0.052	0.002	0.050
Al	0	0.118	0.594	0	1.288
Cr	0	0.002	0.012	0	0.004
Fe	2.427	1.237	1.225	2.103	1.439
Mn	1.548	0.319	0.015	0.042	0.000
Mg	2.889	3.715	3.416	4.985	4.111
Ca	0.252	1.643	1.773	0.054	0.058
Na	0	0.151	0.398	0.024	0.586
K	0	0.027	0.030	0.003	0.004
Total	15.062	15.221	15.515	15.142	15.541
X_{Mg}	0.544	0.750	0.736	0.703	0.741

¹ Manganian. ² In parallel growth. ³ Included in garnet with biotite and quartz in sample HM88011803D. Analysis by M. YATES.

Table 7. Compositions of calcic amphiboles.

Sample	3006	2911A	1317	1317	1317	1317	1911A	1905
Type	Ferro-Prg	Ferroan Prg	Act ¹	Mg-Hbl ¹	Prg-tic Hbl ²	Ferroan Prg ³	Tr	Act
SiO ₂	38.29	38.44	53.20	45.92	43.80	40.11	57.21	54.18
TiO ₂	2.17	0.99	0.01	0.14	0.43	0.20	0.03	0.09
Al ₂ O ₃	10.46	16.90	3.48	10.40	13.28	18.35	0.34	2.85
Cr ₂ O ₃	0.01	0.03	0.01	0.11	0.09	0.12	0.01	0.02
FeO	30.53	13.69	8.57	10.98	10.06	11.28	1.02	5.66
MnO	0.08	0.10	0.09	0.17	0.09	0.19	0.09	0.30
MgO	1.98	11.03	19.45	15.52	15.00	12.27	24.24	20.46
CaO	10.69	12.30	12.29	12.09	12.38	11.44	13.87	13.30
Na ₂ O	1.70	2.09	0.49	1.33	1.63	2.67	0.12	0.30
K ₂ O	1.54	1.01	0.07	0.54	0.81	0.50	0.02	0.14
ZnO	—	0.10	—	—	—	—	0.11	0.13
Total	97.44	96.68	97.65	97.18	97.57	97.12	97.06	97.43
Cations per 23 oxygens								
Si	6.246	5.809	7.530	6.701	6.374	5.908	7.869	7.609
Al	1.754	2.191	0.470	1.299	1.626	2.092	0.056	0.391
Sum	8.000	8.000	8.000	8.000	8.000	8.000	7.925	8.000
Ti	0.266	0.113	0.001	0.015	0.047	0.022	0.003	0.010
Al	0.258	0.820	0.111	0.490	0.652	1.094	0	0.081
Cr	0.001	0.003	0.001	0.013	0.011	0.014	0.001	0.002
Fe	4.165	1.730	1.015	1.340	1.224	1.389	0.117	0.665
Mn	0.010	0.013	0.011	0.020	0.011	0.023	0.011	0.036
Mg	0.482	2.486	4.104	3.376	3.253	2.694	4.970	4.284
Ca	1.869	1.992	1.864	1.891	1.931	1.805	2.044	2.001
Na	0.539	0.612	0.134	0.377	0.460	0.763	0.032	0.081
K	0.320	0.195	0.012	0.100	0.150	0.094	0.004	0.026
Zn	—	0.011	—	—	—	—	0.011	0.013
Total	15.911	15.975	15.252	15.622	15.740	15.899	15.118	15.198
X _{Mg}	0.104	0.590	0.802	0.716	0.727	0.660	0.977	0.866

¹ Zoned grain. ² Matrix. ³ In symplectite around garnet.

Analyses of Ca-poor amphiboles include an orthoamphibole (gedrite) and the clinoamphiboles (typically highly twinned) cummingtonite, which is a common mineral in gneisses lacking K-feldspar and occurs with hornblende and plagioclase in a portion of EG88011317, and tirodite in EG88012807 (Table 6), for which the end member composition is Mn₂Mg₅Si₈O₂₂(OH)₂ (LEAKE, 1978). Tirodite appears to be a later mineral replacing pigeonite and pyroxmangite (Figs. 2 and 3).

Al-poor calcic amphiboles include tremolite, actinolite and manganian actinolite (Tables 6 and 7). In EG88011317 actinolite forms overgrowths on hornblende (Figs. 6 and 18). More aluminous calcic amphiboles show a wide range of composition (Table 7). In sample EG88011317, the least aluminous occur with cummingtonite (Table 6), actinolite, and actinolic hornblende, while the most aluminous are intergrown with anorthite and spinel in symplectites formed from garnet breakdown (Figs. 6 and 18). The ferro-pargasitic hornblende in EG88013006 is dark green; an

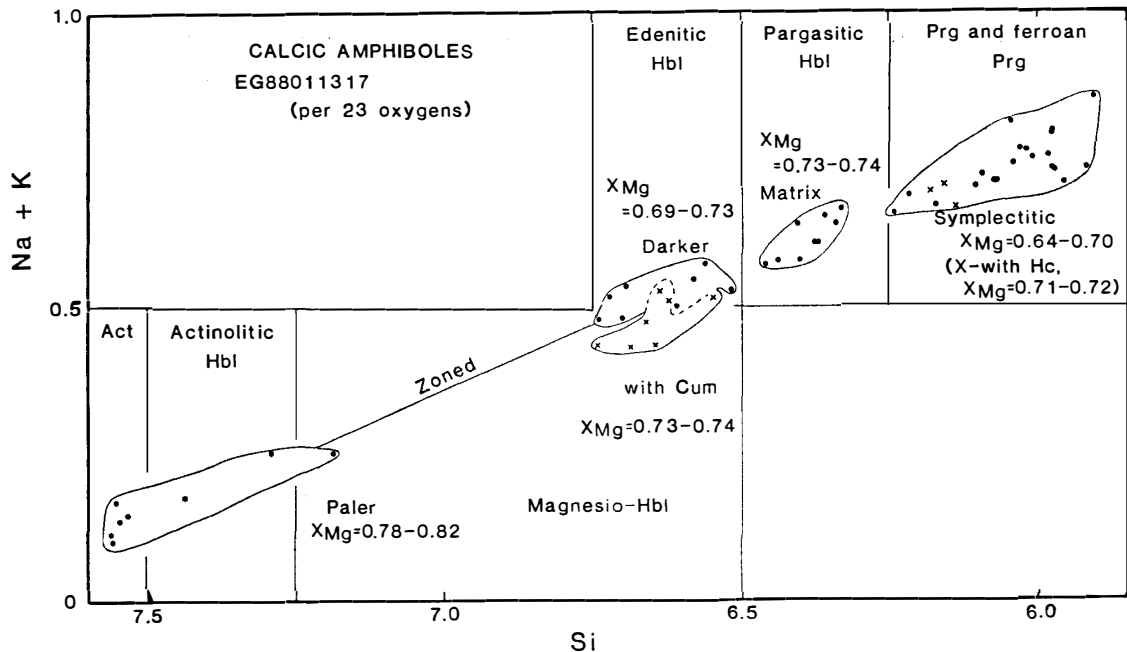


Fig. 18. Plot of calcic amphibole compositions (classification of LEAKE *et al.*, 1978). The line marked "zoned" links the paler margins and darker cores of a single amphibole prism, while the group of x's marked "with Cum" are for calcic amphibole in parallel growth with cummingtonite.

analyzed bluer margin is depleted in Ti (0.4–0.5 wt % TiO_2) and enriched in Al (11.7–11.9 wt % Al_2O_3) compared to the core (similar to composition listed in Table 7).

Biotites range from near end-member phlogopite to an annite-rich variety (Table 8), the latter a late mineral in EG88013006. Secondary muscovite is common, while margarite in fine flakes has been analyzed in EG88012911A (Table 8) and tentatively identified in a few other rocks with little or no quartz. Margarite is associated with hercynite, corundum, magnetite, plagioclase, hornblende, biotite, and chlorite. $\text{Na}/(\text{Na}+\text{Ca}+\text{K})$ ratios in analyzed margarites range 0.10–0.35. Chlorites vary in X_{Mg} and in one grain, marked zoning due to variations in Al/Si ratio (Table 9).

Garnets include varieties rich in spessartine, almandine, and pyrope (Table 10, Fig. 19); garnet grains in the metapelite (EG88011704A) and garnet amphibolite (EG88011317) are markedly zoned, with margins enriched in Fe. The pyrope-rich garnet in EG88011317 is embayed by a symplectite of anorthite, pargasite, and locally, hercynite, suggesting breakdown of a magnesian, calcian garnet component by the following reaction:



A similar reaction (but lacking hercynite) would account for Hbl-Pl symplectites around garnet in the Vesthjelmen amphibolite from which EG88012911A was collected.

Allanite varies considerably in composition (Table 11, Fig. 20). The allanite in EG88011814 is the first to be reported with $\text{Mg}/\text{Fe} > 1$ (DEER *et al.*, 1986; PEACOR and DUNN, 1988), and could be a new mineral species of the epidote group in which

Table 8. Compositions of micas.

Sample	2809	3006	2911A		1317	1704A	1814	1911A	2712B
Mineral	Bt	Ann	Bt	Mrg	Phl	Bt	Phl	Phl	Phl
SiO ₂	37.72	32.64	34.95	30.08	36.78	34.38	38.21	39.80	40.14
TiO ₂	2.33	4.31	1.03	0.02	0.82	2.53	0.85	0.48	1.25
Al ₂ O ₃	15.35	13.47	18.95	50.60	18.04	19.52	16.27	13.64	14.78
Cr ₂ O ₃	0.09	0.03	0.01	0	0.09	0.02	0	0.03	0.05
FeO	13.08	31.88	19.08	1.09	10.28	17.20	1.08	1.45	3.06
MnO	0.49	0.12	0.06	<0.01	0.08	0.09	<0.01	0	0.07
MgO	15.99	2.98	12.00	0.20	18.51	11.19	25.76	28.09	24.00
CaO	0	0.09	0.09	12.04	0.04	0	0.01	0	0.01
Na ₂ O	0.05	0.05	0	0.90	0.61	0.24	0.24	0	0.25
K ₂ O	9.04	8.65	9.40	0.01	8.28	9.29	9.58	10.04	9.54
ZnO	—	—	0.11	0.05	—	0.07	0.01	—	0.21
Sum	94.13	94.21	95.69	94.99	93.53	94.53	92.00	93.52	93.37
Cations per 22 oxygens									
Si	5.639	5.420	5.302	4.018	5.432	5.236	5.526	5.687	5.763
Al	2.361	2.580	2.698	3.982	2.568	2.764	2.474	2.297	2.237
Sum	8.000	8.000	8.000	8.000	8.000	8.000	8.000	7.984	8.000
Ti	0.262	0.538	0.117	0.002	0.091	0.289	0.092	0.051	0.135
Al	0.343	0.056	0.690	3.986	0.571	0.739	0.299	0	0.264
Cr	0.010	0.003	0.001	0	0.011	0.003	0	0.003	0.005
Fe	1.635	4.428	2.420	0.121	1.269	2.191	0.131	0.174	0.367
Mn	0.062	0.017	0.008	0.001	0.010	0.012	0.001	0	0.009
Mg	3.562	0.738	2.713	0.040	4.076	2.541	5.554	5.985	5.137
Zn	—	—	0.013	0.005	—	0.008	0.001	—	0.022
Sum	5.874	5.780	5.962	4.155	6.028	5.783	6.078	6.213	5.939
Ca	0	0.015	0.015	1.723	0.007	0	0.002	0	0.002
Na	0.014	0.017	0	0.233	0.175	0.072	0.066	0.001	0.069
K	1.724	1.832	1.819	0.002	1.560	1.805	1.767	1.829	1.747
Sum	1.738	1.864	1.834	1.958	1.742	1.877	1.835	1.830	1.818
Total	15.611	15.646	15.796	14.113	15.769	15.660	15.911	16.027	15.757
X _{Mg}	0.685	0.143	0.529	0.246	0.763	0.537	0.977	0.972	0.933

the end member (idealized formula CaCeMgAl₂Si₃O₁₂(OH)) is the dominant component. Prof. D. R. PEACOR is currently carrying out a detailed investigation of this material. Clinozoisite and epidote occur not only in calc-silicate rocks (e.g., Table 11), but also as an inclusion in apatite in EG88012911A (Fe₂O₃=7.7–8.1 wt %).

Carbonates include calcite and dolomite in the marbles, rhodochrosite in EG88012807 (65–87 mole % MnCO₃), and manganoan, ferroan dolomite in EG88012809 (8–9% MnCO₃ and 8–11% FeCO₃). Calcite associated with dolomite in marble is magnesian (mostly 2–3 wt % MgO, maximum 3.34%) and in sample EG88011911A, contains abundant exsolution lamellae of dolomite, suggesting greater MgO contents at the highest grade of metamorphism.

Most analyzed ilmenites occurring as independent grains are close to FeTiO₃ with minor Fe₂O₃, which in some cases (e.g. EG88011704A) has partly exsolved as fine hematite lamellae. In sample EG88012911A ilmenite lamellae in magnetite are

Table 9. Compositions of chlorites.

Sample	2911A	1814	1911A		2712B
			Core	Margin	
SiO ₂	25.97	30.07	30.32	32.37	26.81
TiO ₂	0.09	0.06	0.11	0.04	0.03
Al ₂ O ₃	20.91	20.92	19.03	14.59	18.55
Cr ₂ O ₃	0.06	0.01	0	0.06	0
FeO	21.19	1.14	1.54	1.76	25.65
MnO	0.16	0.01	0.06	0.02	0.16
MgO	18.28	32.86	33.27	35.55	13.43
CaO	0.01	0.06	0.04	0.05	0.08
Na ₂ O	0	0	0	0	0
K ₂ O	0	<0.01	0.04	0.01	0.02
ZnO	0	0.02	—	—	0.24
Total	86.68	85.16	84.40	84.43	84.95
Cations per 28 oxygens					
Si	5.417	5.717	5.836	6.242	5.849
Al	2.583	2.283	2.164	1.758	2.151
Sum	8.000	8.000	8.000	8.000	8.000
Ti	0.014	0.009	0.015	0.005	0.005
Al	2.558	2.404	2.154	1.558	2.620
Cr	0.010	0.002	0	0.008	0
Fe	3.696	0.181	0.248	0.284	4.680
Mn	0.028	0.001	0.009	0.002	0.029
Mg	5.685	9.315	9.549	10.220	4.367
Zn	0	0.003	—	—	0.038
Sum	11.991	11.915	11.975	12.077	11.739
Ca	0.002	0.013	0.009	0.010	0.019
Na	0	0	0	0	0
K	0	0.001	0.011	0.003	0.004
Sum	0.002	0.014	0.020	0.013	0.023
Total	19.993	19.930	19.994	20.092	19.762
X _{Mg}	0.606	0.981	0.975	0.973	0.483

typically enriched in MnTiO₃ and somewhat depleted in Fe₂O₃ relative to independent grains enclosed in sphene (*e.g.* Table 12); independent grains in contact with magnetite have intermediate MnTiO₃ contents. In EG88012807 the dominant ilmenite phase is translucent only on thin edges and contains 43–46 mole % MnTiO₃, while rare, transparent brown grains are nearly end-member pyrophanite (Table 12). Magnesian ilmenites are restricted to the marbles; a few grains are properly geikielite ($X_{Mg} > 0.5$, Table 12).

Hercynite is a major constituent of some sillimanite-rich layers in pelitic gneisses, where it forms relatively coarse grains riddled with fine magnetite (Table 13). It also formed from breakdown of garnet (EG88011317) and of magnetite (E688011704A, -2911A). Spinel-hercynite generally contains Zn but little Cr. In marble (EG88011911A) spinel Zn contents are variable and one grain is zoned with cores: 5 wt % (Table 13) and rims: 10–12 wt% ZnO. Zn is the dominant divalent cation

Table 10. Compositions of garnets and kyanite.

Sample	2807	2809	3006	1317		1704A	1803D ¹	
Mineral	Sps	Sps	Alm	Prp	Alm	Alm	Prp	Ky
Location	Core	Core	Core	Core	Rim	Core	Core	
SiO ₂	36.26	36.22	36.48	39.81	38.12	38.80	40.04	36.79
TiO ₂	0.14	0.10	0.03	0.04	0	0	0	0.08
Al ₂ O ₃	19.70	20.57	19.80	23.30	21.92	22.11	22.18	61.46
Cr ₂ O ₃	0	0.03	0.03	0.06	0.05	0	0.22	0.02
FeO	10.98	14.38	33.79	15.41	23.94	28.64	20.35	0.99
MnO	27.39	20.34	1.28	0.33	1.18	0.36	0.40	0.09
MgO	0.94	2.12	0.52	14.22	9.37	8.88	12.79	0.11
CaO	3.60	5.56	7.32	7.35	4.92	1.21	3.80	0
Na ₂ O	<0.01	0	0.04	0	0.01	0.05	—	—
K ₂ O	0	0	0.02	0	0.02	0	—	—
ZnO	—	—	—	—	—	0.09	—	—
Total	99.02	99.32	99.32	100.53	99.54	100.15	99.78	99.54
Cations per 12 oxygens								5 ox.
Si	2.997	2.949	2.997	2.927	2.945	2.992	3.000	1.001
Ti	0.008	0.006	0.002	0.002	0	0	0	0.002
Al	1.919	1.974	1.917	2.019	1.996	2.010	1.960	1.971
Cr	0	0.002	0.002	0.003	0.003	0	0.013	0
Fe	0.759	0.979	2.321	0.948	1.547	1.847	1.276	0.020
Mn	1.918	1.403	0.089	0.021	0.077	0.024	0.024	0.002
Mg	0.115	0.257	0.064	1.559	1.079	1.021	1.427	0.004
Ca	0.319	0.485	0.645	0.579	0.407	0.100	0.303	0
Na	0.001	0	0.006	0	0.002	0.007	—	—
K	0	0	0.002	0	0.002	0	—	—
Zn	—	—	—	—	—	0.005	—	—
Total	8.036	8.056	8.046	8.059	8.058	8.007	8.004	3.001
X _{Mg}	0.132	0.208	0.027	0.622	0.411	0.356	0.528	—

¹ Sample HM88011803D. Analyst, M. YATES. Grt core next to Ky inclusion. Fe in Ky given as Fe₂O₃.

in a gahnite (MA88012305-1, Table 13) associated with sphalerite (8–9% Fe, semi-quantitative analyses, M. YATES).

Högbomite occurs sparingly with hercynite in metapelites (*e.g.* EG88011704A) and in the garnet-amphibolite at Vesthjelmen (*e.g.* EG88012911A). Its composition (Table 13) is somewhat variable in a given section, most notably in ZnO (3.4–6.5 wt %) in EG88011704A.

Sillimanite in EG88011704A contains 0.94–1.12% Fe₂O₃ and 0.05–0.10% Cr₂O₃, consistent with the relatively oxidized conditions indicated by ilmenite composition (GREW, 1980). Identification of kyanite included in garnet was confirmed in one case (HM88011803D, Table 10).

A mineral provisionally identified as a member of the zirconolite group contains 28.6–29.5 wt % TiO₂, 3.0–6.6 wt % FeO, up to 1.3 wt % MnO, 0.2–1.3 wt % MgO, and 5.4–8.4 wt % CaO, as well as significant Y, Zr, Nb, Th and U (qualitative analyses). Other secondary minerals include fluorite as blebs in scapolite (confirmed

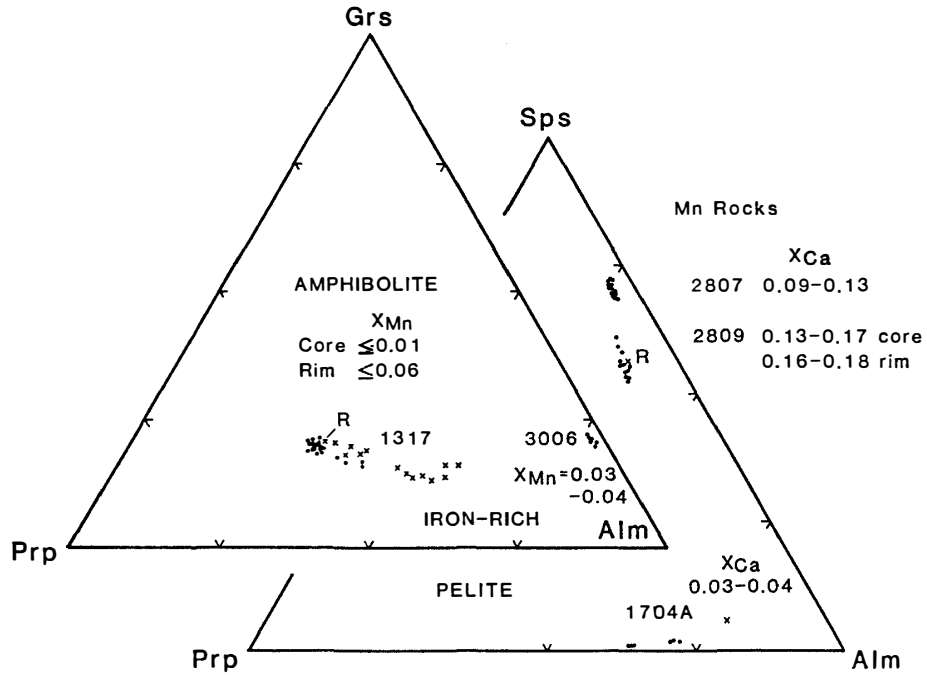


Fig. 19. Plot of garnet compositions for five samples (prefix EG8801-). Filled circles are core compositions, x's are rim compositions, in places indicated by R. $X_{Mn} = Mn / (Mn + Fe + Mg + Ca)$ and $X_{Ca} = Ca / (Ca + Mn + Mg + Fe)$.

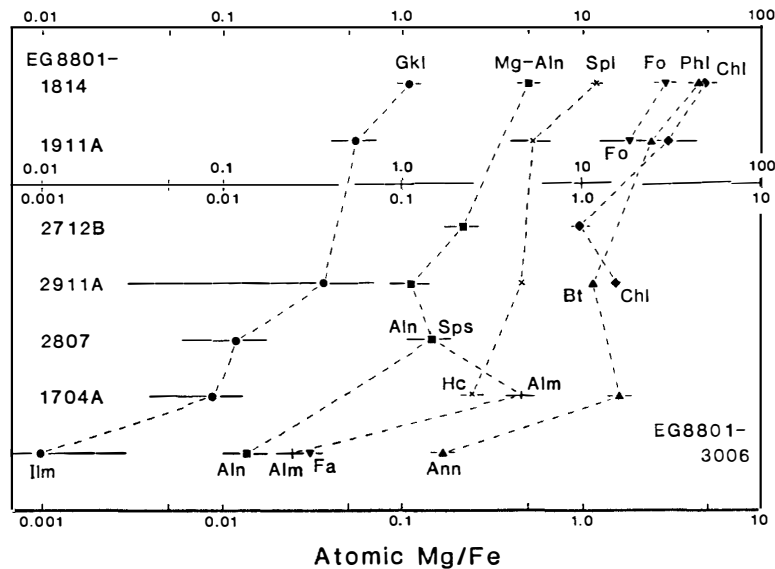


Fig. 20. Logarithmic plot of atomic Mg/Fe ratios of ferromagnesian minerals in 7 samples. Adopted from ALBEE (1968). The samples are listed in a sequence of increasing Mg/Fe ratio upwards. The horizontal lines represent the range of Mg/Fe ratios measured on a given mineral in each sample; the symbol is at the median value.

by qualitative analysis in EG88012712B) and rarely in biotite in calc-silicate rocks and tourmaline as rare grains in the Vesthjelmen garnet amphibolite and in a veinlet from northern Balchen Mountain (Fig. 1). Secondary prehnite occurs with mus-

Table 11. Compositions of allanites and clinozoisite.

Sample	2807	3006	2911A	1814	2712B		1905
Mineral	Aln	Aln	Aln	Aln	Aln	Czo	Czo
SiO ₂	28.10	29.36	33.16	29.90	31.57	38.53	38.94
TiO ₂	3.36	1.20	0.36	1.06	0.13	0.03	0
Al ₂ O ₃	9.08	13.25	19.26	14.51	18.41	28.57	33.13
Cr ₂ O ₃	0	0	0	0.01	0	0	0
FeO	10.13	16.51	7.95	2.08	8.29	6.50 ¹	0.35 ¹
MnO	5.22	0	0.29	0	0	0.02	0.28
MgO	0.91	0.14	0.62	5.64	1.00	0.09	0.05
CaO	7.30	11.40	14.83	11.98	16.33	24.25	24.63
Na ₂ O	0	0	0.15	0	0	0	0
K ₂ O	0.04	0	0.01	0.02	0.02	0	0
ZnO	—	—	0.04	0.09	0.08	0.07	0.28
Total	64.13	71.86	76.66	65.28	75.82	98.07	97.66
	Cations normalized to 3Si (All Fe=Fe ²⁺)				12.5 oxygens (All Fe=Fe ³⁺)		
Si	3.000	3.000	3.000	3.000	3.000	2.989	2.972
Ti	0.270	0.092	0.024	0.080	0.009	0.002	0
Al	1.143	1.596	2.054	1.716	2.062	2.612	2.981
Cr	0	0	0	0.001	0	0	0
Fe	0.904	1.411	0.602	0.175	0.659	0.380	0.020
Mn	0.472	0	0.022	0	0	0.001	0.018
Mg	0.145	0.021	0.083	0.844	0.142	0.010	0.006
Ca	0.835	1.248	1.438	1.287	1.662	2.016	2.015
Na	0.000	0	0.027	0	0	0	0
K	0.005	0	0.001	0.002	0.002	0	0
Zn	—	—	0.002	0.007	0.006	0.004	0.016
Total	6.774	7.368	7.253	7.111	7.542	8.014	8.027
X _{Mg}	0.138	0.014	0.121	0.829	0.177	—	—

¹ Fe as Fe₂O₃.

covite in scapolite in EG88011905 (one analysis gave 43.0 wt % SiO₂, 24.5 wt % Al₂O₃, 27.5 wt % CaO and 95.1% Sum, 11 elements).

4. Chemical Relations among the Minerals

With the exception of sample EG88013006, the compositions of the minerals in any given sample are variable. This observation supports the textural evidence for a complex metamorphic history. Nonetheless, Fe-Mg distribution among associated minerals follows broad trends indicative of approach to equilibrium. On a logarithmic plot of Mg/Fe ratios (Fig. 20), the sequence of increasing Mg/Fe ratios for ferromagnesian minerals is with a few exceptions the same for 7 samples, while the distances between the plotted points are similar, resulting in roughly parallel lines. These features suggest that chemical equilibrium had in many cases been approached (ALBEE, 1968), although there is little evidence for textural equilibrium in these rocks (except EG88013006).

Table 12. Compositions of ilmenites.

Sample	2807		3006	2911A		1704A	1814	1911A
	Prn ¹	Ilm ¹	Ilm ¹	Ilm ¹	Ilm ²	Ilm ^{1,3}	Gkl ¹	Ilm ¹
SiO ₂	0.04	0	0	0	0	0	0.05	<0.01
TiO ₂	51.89	52.54	51.39	51.15	52.16	50.16	59.84	57.35
Al ₂ O ₃	0.01	0.05	0.08	0	0.06	0.04	0.01	0
Cr ₂ O ₃	0	0	0.02	0	0	0.14	0.11	0
FeO	1.85	25.48	48.42	45.17	41.97	48.74	23.35	29.30
MnO	44.60	21.07	0.34	1.24	5.12	0.57	0.65	3.13
MgO	0.01	0.09	0.01	1.76	0.68	0.14	16.46	11.07
CaO	0.08	0.02	0.01	0.01	0	0.03	0.06	0.06
Na ₂ O	0	0	0.09	0	0	0.01	0	0.03
K ₂ O	0	0	0	0	0.02	0.02	0	0
ZnO	—	0.09	—	0	0	0.18	0	—
Total	98.48	99.34	100.36	99.31	100.02	100.01	100.53	100.95
Cations per 6 oxygens								
Si	0.002	0	0	0	0	0	0.002	0
Ti	1.991	2.001	1.943	1.926	1.968	1.899	2.001	1.988
Al	0.001	0.003	0.005	0	0.004	0.002	0	0
Cr	0	0	0.001	0	0	0.005	0.004	0
Fe ³⁺	—	0	0.108	0.149	0.061	0.194	0	0.024
Fe ²⁺	0.079	1.079	1.928	1.742	1.699	1.858	0.868	1.105
Mn	1.928	0.904	0.015	0.052	0.217	0.024	0.025	0.122
Mg	0.001	0.007	0.001	0.131	0.051	0.010	1.091	0.761
Ca	0.004	0.001	—	0	0	—	0.003	—
Zn	—	0.003	—	0	0	0.007	0	—
Total	4.006	3.998	4.0 ⁺	4.0 ⁺	4.0 ⁺	4.0 ⁺	3.995	4.0 ⁺
X _{Mg}	0.012	0.006	0.000	0.065	0.028	0.005	0.557	0.402

¹ Independent grain. ² Lamella in magnetite. ³ Fine exsolution lamellae of hematite.
⁴ Normalized to 4 cations and Fe³⁺ calculated by stoichiometry. Si, Ca, Na, K contents ignored.
X_{Mg} is given in terms of total Fe.

Figure 20 also provides an explanation for the unusual magnesian enrichment in the secondary minerals in the marbles (EG88011814, -1911A). Ilmenite and allanite have the lowest Mg/Fe ratios, consistently lower than those for the generally iron-rich minerals, garnet and spinel-hercynite. Consequently, only in highly magnesian assemblages, in which even Spl X_{Mg} exceeds 0.9, will ilmenite and allanite X_{Mg} exceed 0.5.

5. Pressure-Temperature Estimates

Field data, thin section petrography, and microprobe analyses clearly demonstrate that the eastern Sør Rondane Mountains is a terrain of multiple metamorphism. Our observations suggest that the rocks are affected by at least two events, (1) an early high-grade event ranging from the amphibolite facies (Hettene, Austhjellen, Vesthjellen) to the granulite facies (Austhamaren and the exposures

Table 13. Compositions of spinels and högbomite.

Sample	2911A	1317	1704A	1814	1911A	2305-1	2911A	1704A
Mineral	Hc	Hc	Hc	Spl	Spl	Ghn ¹	Hög	Hög
SiO ₂	0	0	0	0.05	0	—	0	0
TiO ₂	0.07	0	0	0.03	0	0	7.43	4.34
Al ₂ O ₃	59.43	59.29	57.98	69.70	66.00	53.63	57.62	59.04
Cr ₂ O ₃	0	0.95	0.76	0.06	0.07	0.27	0.03	0.59
FeO	26.66	29.05	30.07	3.48	8.75	10.89	24.13	23.78
MnO	0.77	0.14	0.14	0	0.09	0.20	0.56	0.07
MgO	6.57	8.48	4.54	25.42	20.54	1.23	5.19	2.66
CaO	0.05	0.04	0.02	0.03	0.01	—	<0.01	0
K ₂ O	0	0.00	0	0	<0.01	—	0.02	0
ZnO	6.56	1.08	5.70	0.66	5.44	33.26	2.66	6.46
Total	100.11	99.02	99.19	99.42	100.91	99.48	97.65	96.95
	Cations per 4 oxygens					31 Oxygens		
Si	0	0	0	—	0	—	0	0
Ti	0.002	0	0	0.001	0	0	1.208	0.721
Al	1.951	1.933	1.949	1.995	1.947	1.914	14.677	15.376
Cr	0	0.021	0.017	0.001	0.001	0.006	0.005	0.103
Fe ³⁺	0.045	0.047	0.034	0.002	0.052	0.080	—	—
Fe ²⁺	0.576	0.625	0.684	0.068	0.131	0.196	4.361	4.395
Mn	0.018	0.003	0.003	0	0.002	0.005	0.102	0.013
Mg	0.273	0.349	0.193	0.920	0.766	0.056	1.673	0.878
Zn	0.135	0.022	0.120	0.012	0.101	0.743	0.425	1.054
Total	3.0 ²	3.0 ²	3.0 ²	3.0 ²	3.0 ²	3.0 ²	22.451	22.540
X _{Mg}	0.305	0.342	0.212	0.929	0.807	0.168	0.277	0.166

¹ Sample MA88012305-1, Analyst, M. YATES. V below detection limit.

² Normalized to 3 cations and Fe³⁺ calculated by stoichiometry. Si, Ca, Na, K contents ignored (also in Hög formulae). X_{Mg} in terms of total Fe.

south of it) and (2) a later amphibolite-facies event associated with migmatization (ASAMI *et al.*, 1989). A magmatic event, presently represented by the biotitic schist metadikes, intervened between events (1) and (2), indicating that these two events are discrete. The entire area was affected by retrogression in the greenschist facies, which could have resulted from activity on the retrograde path of the amphibolite facies event or from a separate event (or both). In view of the widespread development of non-equilibrium textural and chemical features, calculations of temperatures and pressures based on mineral compositions should be considered with caution.

Sample EG88013006 contains two assemblages useful for estimating pressure for the earlier event: Fs-Fa (BOHLEN and BOETTCHER, 1981) and Pl-Grt-Ol (BOHLEN *et al.*, 1983). The most iron rich ferrosilites, which average $\text{Fs}_{88.0}\text{Rdn}_{1.3}\text{En}_{0.0}\text{Wo}_{1.7}$, (e.g. Table 5) indicate pressures of 7 kbar (at 700°C) (see also NEWTON, 1983); this value is a minimum as quartz is absent. From an assemblage of neighboring grains that would give maximum values of the pressure from Pl-Grt-Ol, that is plagioclase ($X(\text{An})=0.1010$, Table 3), garnet ($X(\text{Ca})=0.2213$, $X(\text{Fe})=0.7582$, $X(\text{Mg})=0.0205$), and fayalite ($X(\text{Fe})=0.973$, Table 4), with the activity models listed in BOHLEN *et al.*

Table 14. Selected estimates of temperature.

Sample No. EG8801-	Garnet-Clinopyroxene				Temperature ¹ °C (at 7 kbar)	
	Grt X_{Mg}	Grt X_{Ca}	Cpx X_{Mg}	ln K	EG	PN ($X_{Ca}=0.2$)
1317	0.541	0.166	0.747	0.9203	1009	867
1317	0.622	0.188	0.798	0.8784	1053	911
3006	0.027	0.213	0.134	1.7216	766	<700
	Garnet-Orthopyroxene			ln K	HG	SB
3006	Grt X_{Mg}	Opx X_{Mg}				
	0.027	0.094	1.3233	642	721	
	Orthopyroxene-Clinopyroxene			ln K	WB	W
3006	Cpx X_{Mg}	Opx X_{Mg}				
	0.134	0.095	1.474	780	777	
	Garnet-Biotite		ln K	T	FS	PL
1317	Grt X_{Mg}	Bt X_{Mg}				
	0.622	0.763	-0.6694	960	1212	839
1317	0.436 ²	0.772 ²	-1.4782	627	681	632
3006	0.028	0.143 ³	-1.7610	550	575	577
1704A	0.180 ²	0.531	-1.6419	581	616	599
	CaCO ₃ Scapolite-Plagioclase			GOLDSMITH & NEWTON (1977)		
1905	Scp X_{Ca}	Pl X_{Ca}				
	0.763	0.944			702	
1905	0.746	0.932			680	
	Calcite-Dolomite		ANOVITZ & ESSENE (1987)			
1911A	Cal X_{Mg}					
	0.078				620	
1814	0.057				552	

¹ Abbreviations: EG—ELLIS and GREEN (1979), PN—PATTISON and NEWTON (1989), HG—HARLEY (1984), SB—SEN and BHATTACHARYA (1984), WB—WOOD and BANNO (1973), W—WELLS (1977), T—THOMPSON (1976), FS—FERRY and SPEAR (1978), PL—PERCHUK and LAVRENT'eva (1983); ² Margins; ³ Secondary.

(1983, Table 3), $K_D=0.694$ and $P=9$ kbar (at 700°C). Other plagioclase grains are more calcic (to An₁₆), and would give lower pressures. In sum, the data on sample EG88013006 yield a conservative pressure estimate of 7 kbar for the early metamorphic event. This estimate is consistent with the absence of cordierite in the metapelites ($P>7$ kbar, NEWTON, 1983, Fig. 5) and the presence of relict kyanite, which implies pressures above the Al₂SiO₅ triple point (4 kbar, HOLDAWAY, 1971) during the prograde path of the earlier event. Evidence for high pressures during the prograde path in the granulite-facies rocks is pyropic garnet with inclusions of kyanite and gedrite (sample HM88011803D), which could be relics of a former Ky-Ged±Qtz assemblage (≥ 6 kbar, SCHREYER and SEIFERT, 1969; GREEN and VERNON, 1974). The formation of pyropic garnet from Ky-Ged (reactions 2-3) may require an increase in pressure as well as temperature.

Table 14 summarizes the maximum temperatures calculated from individual analyses of neighboring grains in several samples by a variety of methods. Many

of the temperatures calculated for sample EG88013006 using the five pre-1989 garnet-pyroxene and pyroxene-pyroxene geothermometers listed in Table 14 range from 700 to 780°C, which are "reasonable" for granulite-facies metamorphism and consistent with formation of orthopyroxene in gneisses from Austhamaren. However, the validity of most of these geothermometers has been questioned (*e.g.*, BOHLEN and ESSENE 1979; PATTISON and NEWTON, 1989). The "reasonable" values could be spurious and the PATTISON and NEWTON (1989) values below 700°C could be post-granulite facies closure or resetting temperatures.

Temperatures calculated from garnet cores, matrix biotite, and clinopyroxene in EG88011317 are unrealistically high, possibly because the garnet cores, being relics of a relatively high-pressure prograde path, never had equilibrated with the present compositions of clinopyroxene and biotite.

Garnet-rim-biotite (in part clearly secondary) and maximum calcite Mg contents give temperatures in the 450–630°C range. The higher values are reasonable for the amphibolite-facies event.

The scapolite-plagioclase temperatures near 700°C would apply to the formation of metasomatic silicate veins cutting marbles and apparently related to pegmatites, that is, presumably to the amphibolite-facies event.

6. Conclusion

Our findings indicate that much of the eastern Sør Rondane Mountains had been affected by a granulite-facies event and subsequently recrystallized under amphibolite-facies conditions, consistent with RAVICH and KAMENEV's (1972) interpretation. Kyanite inclusions in plagioclase and garnet imply a prograde path at pressures above 4 kbar, which are also suggested by magnesian cores in garnet; this led to peak conditions estimated to be ≥ 7 kbar and 700–750°C. Kyanite petrogenesis in the eastern Sør Rondane Mountains differs from that in western Sør Rondane Mountains, where kyanite occurs as a later formed mineral in biotite (ASAMI and SHIRAIISHI, 1987), but is analogous to that on the Prince Olav and Sôya Coasts, where kyanite relics are characteristic of the Lützow-Holm Bay Complex (HIROI *et al.*, 1983; MOTOYOSHI *et al.*, 1985).

Acknowledgments

The authors thank the other members of the Sør Rondane survey party and of JARE-29 for their kind support during the field work, Mr. H. KOJIMA and Dr. Y. MOTOYOSHI for their assistance with operation of the microprobe at the National Institute of Polar Research and Dr. M. YATES for the microprobe analyses at the University of Maine. E.S.G. thanks Dr. K. SHIRAIISHI and other staff at the Institute for their generous support during his six-month stay as invited scientist. E.S.G.'s research was funded by the National Institute of Polar Research and by U.S. National Science Foundation grant DPP8613241 (to the University of Maine).

References

- ALBEE, A. L. (1968): Metamorphic zones in northern Vermont. *Studies of Appalachian Geology; Northern and Maritime*, ed. by E. ZEN *et al.* New York, Interscience, 329–341.
- ANOVITZ, L. M. and ESSENE, E. J. (1987): Phase equilibria in the system $\text{CaCO}_3\text{-MgCO}_3\text{-FeCO}_3$. *J. Petrol.*, **28**, 389–414.
- ASAMI, M. and SHIRAIISHI, K. (1987): Kyanite from the western part of the Sør Rondane Mountains, East Antarctica. *Proc. NIPR Symp. Antarct. Geosci.*, **1**, 150–168.
- ASAMI, M., MAKIMOTO, H. and GREW, E. S. (1989): Geology of the eastern Sør Rondane Mountains, East Antarctica. *Proc. NIPR Symp. Antarct. Geosci.*, **3**, 81–99.
- BOHLEN, S. R. and ESSENE, E. J. (1979): A critical evaluation of two-pyroxene thermometry in Adirondack granulites. *Lithos*, **12**, 335–345.
- BOHLEN, S. R. and BOETTCHER, A. L. (1981): Experimental investigations and geological applications of orthopyroxene geobarometry. *Am. Mineral.*, **66**, 951–964.
- BOHLEN, S. R., WALL, V. J. and BOETTCHER, A. L. (1983): Experimental investigation and application of garnet granulite equilibria. *Contrib. Mineral. Petrol.*, **83**, 52–61.
- BONNICHSEN, B. (1969): Metamorphic pyroxenes and amphiboles in the Biwabik Iron Formation, Dunka River Area, Minnesota. *Mineral. Soc. Am. Spec. Pap.*, **2**, 217–239.
- DEER, W. A., HOWIE, R. A. and ZUSSMAN, J. (1982): *Rock-Forming Minerals*, volume 1A (2nd ed.). Orthosilicates. London, Longman, 919 p.
- DEER, W. A., HOWIE, R. A. and ZUSSMAN, J. (1986): *Rock-Forming Minerals*, volume 1B (2nd ed.). Disilicates and Ring Silicates. New York, Longman and J. Wiley, 629 p.
- ELLIS, D. J. and GREEN, D. H. (1979): An experimental study of the effect of Ca upon garnet-clinopyroxene Fe-Mg exchange equilibria. *Contrib. Mineral. Petrol.*, **71**, 13–22.
- FERRY, J. M. and SPEAR, F. S. (1978): Experimental calibration of the partitioning of Fe and Mg between biotite and garnet. *Contrib. Mineral. Petrol.*, **66**, 113–117.
- FROST, B. R. (1973): Ferroan gahnite from quartz-biotite-almandine schist, Wind River Mountains, Wyoming. *Am. Mineral.*, **58**, 831–834.
- GOLDSMITH, J. R. and NEWTON, R. C. (1977): Scapolite-plagioclase stability relations at high pressures and temperatures in the system $\text{NaAlSi}_3\text{O}_8\text{-CaAl}_2\text{Si}_2\text{O}_7\text{-CaCO}_3\text{-CaSO}_4$. *Am. Mineral.*, **62**, 1063–1081.
- GREEN, T. H. and VERNON, R. H. (1974): Cordierite breakdown under high-pressure, hydrous conditions. *Contrib. Mineral. Petrol.*, **46**, 215–226.
- GREW, E. S. (1980): Sillimanite and ilmenite from high-grade metamorphic rocks of Antarctica and other areas. *J. Petrol.* **21**, 39–68.
- GREW, E. S., ASAMI, M. and MAKIMOTO, H. (1988): Field studies in the eastern Sør Rondane Mountains, East Antarctica, with the 29th Japanese Antarctic Research Expedition (JARE). *Antarct. J. U.S.*, **23**(5), 44–46.
- HARLEY, S. L. (1984): An experimental study of the partitioning of Fe and Mg between garnet and orthopyroxene. *Contrib. Mineral. Petrol.*, **86**, 359–373.
- HIROI, Y. and KOJIMA, H. (1988): Petrology of dolomitic marbles from Kasumi Rock, Prince Olav Coast, East Antarctica. *Proc. NIPR Symp. Antarct. Geosci.*, **2**, 96–109.
- HIROI, Y., SHIRAIISHI, K., YANAI, K. and KIZAKI, K. (1983): Aluminum silicates in the Prince Olav and Sôya Coasts, East Antarctica. *Mem. Natl Inst. Polar Res., Spec. Issue*, **28**, 115–131.
- HOLDAWAY, M. J. (1971): Stability of andalusite and the aluminum silicate phase diagram. *Am. J. Sci.*, **271**, 97–131.
- KATSUSHIMA, T. (1985): Granulite-facies rocks in several islands west of Langhovde, East Antarctica. *Mem. Natl Inst. Polar Res., Spec. Issue*, **37**, 95–110.
- KOBAYASHI, H. (1977): Kanoite, $(\text{Mn}^{2+}, \text{Mg})_2[\text{Si}_2\text{O}_6]$, a new clinopyroxene in the metamorphic rock from Tatehira, Oshima Peninsula, Hokkaido, Japan. *J. Geol. Soc. Jpn.*, **83**, 537–542.
- KRETZ, R. (1983): Symbols for rock-forming minerals. *Am. Mineral.*, **68**, 277–279.
- LEAKE, B. E. (1978): Nomenclature of amphiboles. *Am. Mineral.*, **63**, 1023–1052.
- MORIMOTO, N., FABRIES, J., FERGUSON, A. K., GINZBURG, I. V., ROSS, M., SEIFERT, F. A. *et al.* (1988): Nomenclature of pyroxenes. *Am. Mineral.*, **73**, 1123–1133.

- MOTOYOSHI, Y., MATSUBARA, S., MATSUEDA, H. and MATSUMOTO, Y. (1985): Garnet-sillimanite gneisses from the Lützow-Holm Bay region, East Antarctica. *Mem. Natl Inst. Polar Res., Spec. Issue*, **37**, 82-94.
- NEWTON, R. C. (1983): Geobarometry of high-grade metamorphic rocks. *Am. J. Sci.*, **283-A**, 1-28.
- PATTISON, D. R. M. and NEWTON, R. C. (1989): Reversed experimental calibration of the garnet-clinopyroxene Fe-Mg exchange thermometer. *Contrib. Mineral. Petrol.*, **101**, 87-103.
- PEACOR, D. R. and DUNN, P. J. (1988): Dollaseite-(Ce) (magnesium orthite redefined); Structure refinement and implications for $F+M^{2+}$ substitutions in epidote-group minerals. *Am. Mineral.*, **73**, 838-842.
- PERCHUK, L. L. and LAVRENT'eva, I. V. (1983): Experimental investigation of exchange equilibria in the system cordierite-garnet-biotite. *Kinetics and Equilibrium in Mineral Reactions*, ed. by S. K. SAXENA. New York, Springer-Verlag, 199-239.
- PETERSEN, E. U., ANOVITZ, L. M. and ESSENE, E. J. (1984): Donpeacorite, $(Mn, Mg)MgSi_2O_6$, a new orthopyroxene and its proposed phase relations in the system $MnSiO_3$ - $MgSiO_3$ - $FeSiO_3$. *Am. Mineral.*, **69**, 472-480.
- RAVICH, M. G. and KAMENEV, YE. N. (1972): *Kristallicheskiy Fundament Antarkticheskoy Platformy (Crystalline Basement of the Antarctic Platform)*. Leningrad, Gidrometeoizdat, 658 p.
- SCHREYER, W. and SEIFERT, F. (1969): Compatibility relations of the aluminum silicates in the systems MgO - Al_2O_3 - SiO_2 - H_2O and K_2O - MgO - Al_2O_3 - SiO_2 - H_2O at high pressures. *Am. J. Sci.*, **267**, 371-388.
- SEN, S. K. and BHATTACHARYA, A. (1984): An orthopyroxene-garnet thermometer and its application to the Madras charnockites. *Contrib. Mineral. Petrol.*, **88**, 64-71.
- THOMPSON, A. B. (1976): Mineral reactions in pelitic rocks; II. Calculation of some P-T-X (Fe-Mg) phase relations. *Am. J. Sci.*, **276**, 425-454.
- TRACY, R. J., LINCOLN, T. N., ROBINSON, P. and ASHENDEN, D. D. (1980): Rhodonite-pyroxmangite-pyroxene-amphibole assemblages. *EOS; Trans. Am. Geophys. Union*, **61**, 390-391
- WELLS, P. R. A. (1977): Pyroxene thermometry in simple and complex systems. *Contrib. Mineral. Petrol.*, **62**, 129-139.
- WOOD, B. J. and BANNO, S. (1973): Garnet-orthopyroxene and orthopyroxene-clinopyroxene relationships in simple and complex systems. *Contrib. Mineral. Petrol.*, **42**, 109-124.
- YATES, M. G. and HOWD, F. H. (1988): Contact metamorphism of the Black Hawk Zn-Pb-Cu Deposit, Hancock Co., Maine. *Marit. Sediments Atl. Geol.*, **24**, 267-279.

(Received March 22, 1989; Revised manuscript received May 17, 1989)